Published in final edited form as:
Cell Mol Life Sci. 2014 December ; 71(24): 4853–4867. doi:10.1007/s00018-014-1647-7.

TRPM6 kinase activity regulates TRPM7 trafficking and inhibits cellular growth under hypomagnesic conditions

Katherine Brandao[1], **Francina Deason-Towne**[1,3], **Xiaoyun Zhao**[1,2], **Anne-Laure Perraud**[1,2,§], and **Carsten Schmitz**[1,§]

[1]Integrated Department of Immunology, University of Colorado School of Medicine, 1400 Jackson Street, Denver, CO, 80206, USA

[2]National Jewish Health, 1400 Jackson Street, Denver, CO, 80206, USA

[3]Department of Biology, Regis University, 3333 Regis Boulevard, Denver, CO 80221, USA

Abstract

The channel kinases TRPM6 and TRPM7 are both members of the melastatin related transient receptor potential (TRPM) subfamily of ion channels and the only known fusions of an ion channel pore with a kinase domain. TRPM6 and TRPM7 form functional, tetrameric channel complexes at the plasma membrane by heteromerization. TRPM6 was previously shown to cross-phosphorylate TRPM7 on threonine residues, but not vice versa. Genetic studies demonstrated that TRPM6 and TRPM7 fulfill non-redundant functions, and that each channel contributes uniquely to the regulation of Mg^{2+} homeostasis. Although there are indications that TRPM6 and TRPM7 can influence each other's cellular distribution and activity, little is known about the functional relationship between these two channel-kinases.

In the present study, we examined how TRPM6 kinase activity influences TRPM7 serine phosphorylation, intracellular trafficking, and cell surface expression of TRPM7, as well as Mg^{2+}-dependent cellular growth. We found TRPM7 serine phosphorylation via the TRPM6 kinase, but no TRPM6 serine phosphorylation via the TRPM7 kinase. Intracellular trafficking of TRPM7 was altered in HEK-293 epithelial kidney cells and DT40 B cells in the presence of TRPM6 with intact kinase activity, independently of the availability of extracellular Mg^{2+}, but TRPM6/7 surface labeling experiments indicate comparable levels of the TRPM6/7 channels at the plasma membrane. Furthermore, using a complementation approach in TRPM7-deficient DT40 B-cells, we demonstrated that wildtype TRPM6 inhibited cell growth under hypomagnesic cell culture conditions in cells co-expressing TRPM6 and TRPM7, however co-expression of a TRPM6 kinase dead mutant had no effect – a similar phenotype was also observed in TRPM6/7 co-expressing HEK-293 cells.

Our results provide first clues about how heteromer formation between TRPM6 and TRPM7 influences the biological activity of these ion channels. We show that TRPM6 regulates TRPM7 intracellular trafficking and TRPM7 dependent cell growth. All these effects are dependent upon the presence of an active TRPM6 kinase domain.

Corresponding authors: Carsten Schmitz, Contacts: Phone: 303-270-2732, Fax: 303-270-2325, carsten.schmitz@ucdenver.edu, Anne-Laure Perraud, Phone: 303-270-2078, Fax: 303-270-2325, perrauda@njhealth.org.
[§]Both authors contributed equally to this work

Dysregulated Mg^{2+}-homeostasis causes or exacerbates many pathologies. As TRPM6 and TRPM7 are expressed simultaneously in numerous cell types, understanding how their relationship impacts regulation of Mg^{2+}-uptake is thus important knowledge.

Keywords

Magnesium (Mg^{2+}); Calcium (Ca^{2+}); TRPM6; TRPM7; alpha-kinase

1. Introduction

Regulation of Mg^{2+} homeostasis is a critical component to maintaining cellular growth and division. Two members of the TRPM (Transient Receptor Potential Melastatin) subfamily of cationic ion channels, TRPM6 (Chak2) and TRPM7 (TRP-PLIK, ChaK1, and LTRPC7), have been implicated in regulating Mg^{2+} levels in various cellular contexts. Both TRPM6 and TRPM7 are Ca^{2+} and Mg^{2+} permeable ion channels with similar biophysical properties [1-3], but TRPM7 is ubiquitously expressed whereas TRPM6 has a much narrower cellular expression pattern. TRPM6 is mainly present in kidney, intestine and lung [4, 5], although recent studies indicate that TRPM6 might have a broader expression pattern, specifically in cells of the immune system [6]. These studies highlight the need to better understand the biological relevance of these two channels and their reciprocal relationship. While TRPM6 and TRPM7 are functionally non-redundant and neither can compensate for the other's deficiency in humans (TRPM6 deficiency in HSH patients)[4, 5], in mice ($TRPM6^{-/-}$ or $TRPM7^{-/-}$ mice) [7-9], or in chicken DT40 B-lymphocytes ($TRPM7^{-/-}$ DT40 B cells)[10], we previously found that TRPM7 facilitates TRPM6 plasma membrane localization, and that TRPM6 kinase crossphosphorylates TRPM7 on threonine residues [11].

TRPM6 and TRPM7 stand out as the only known fusions between an ion pore and a serine / threonine kinase domain. Both kinase domains, localized at the cytosolic C-terminus of the ion channels, share 75% protein sequence identity and belong to the atypical alpha kinase family [12]. The crystal structure of TRPM7 kinase shows strong similarities to Protein Kinase A (PKA) [13], despite an absence of protein sequence homology. Both the TRPM6 and TRPM7 kinase domains have similar physiological characteristics regarding their ion and nucleotide dependence [14]. Although the intrinsic kinase domain of TRPM7 is not essential for channel gating [10, 15], its activity has been reported to modulate TRPM7 channel function [10].

While TRPM6 and TRPM7 are able to build heteromultimers [16], and share many biophysical and biochemical properties, their kinases do not have identical substrate specificities. We found TRPM6 and TRPM7 both autophosphorylate threonine residues, but only TRPM6 crossphosphorylates TRPM7, and not the reverse [11]. *In vitro* phosphorylation studies by different groups led to the discovery of several TRPM7 kinase substrates, including annexin I [17], myosin II (also phosphorylated by TRPM6 kinase) [18], eukaryotic Elongation Factor 2 kinase (eEF2K) [19] and Phospholipase C gamma 2 (PLCγ2) [20]. TRPM7's phosphotransferase activity may regulate the activity of its channel domain in accordance to the environmental availability of Mg^{2+}, as the inhibitory phosphorylation of eEF2K via TRPM7 increases under hypomagnesic cell culture conditions [19].

Mutations and deletions of both TRPM6 and TRPM7 cause profound cellular dysfunction and are often lethal, indicative of the important role these channels play in regulating Mg^{2+} homeostasis. TRPM6 mutations in humans have been linked to an autosomal recessive form of familiar hypomagnesemia with secondary hypocalcemia (HSH). These patients fail to build a functional TRPM6 pore and suffer from neurological symptoms, including seizures and muscle spasms during infancy, and eventually die if not treated by Mg^{2+} supplementation [4, 5]. Over the last decade numerous studies have demonstrated that TRPM7 plays an important role in cell proliferation ([21], reviewed in [6]), cell migration [22], protein translation [19], immuno receptor signaling [20], cytoskeleton building (reviewed in [23, 24], cancer development (reviewed in [25]) and cancer metastasis [26].

TRPM6 and TRPM7 knock out mice ($TRPM6^{-/-}$ and $TRPM7^{-/-}$) are both embryonically lethal [7-9, 27]. Mice with inducible, T cell restricted TRPM7 deletion show a block in thymocyte development at the double negative stage and a depletion of thymic medullary cells, but no measureable changes in intracellular Ca^{2+} or Mg^{2+} concentrations ([7], reviewed in [6, 28]). However, in another study the same research group excluded any role for TRPM7 kinase in Fas induced apoptosis in $TRPM7^{-/-}$ T-cells ([29], reviewed in [28]). Future studies will need to clarify whether this developmental phenotype is T cell specific, or if TRPM7 is such an essential gene that its absence is causing decreased viability and developmental failures in any cellular context. Homozygous TRPM7 kinase deletion mutants generated by Ryazanova and colleagues [8] are embryonically lethal as well, whereas the corresponding heterozygote mice are viable, but hypomagnesic, and exhibit reduced intestinal Mg^{2+} absorption [8]. The same group were able to rescue TRPM7 kinase deficient embryonic stem cells going into growth arrest by additional Mg^{2+} supplementation [8]. In analogy, TRPM7 deficient chicken DT40 B-cells go into cell-growth arrest and die under physiological levels of Mg^{2+} (~1mM), but grow normally if the medium is supplemented with 5-10 mM Mg^{2+}. $TRPM7^{-/-}$ DT40 cells can be rescued by overexpression of human TRPM7 WT, TRPM7 kinase dead mutants [10], and partially by the human Mg^{2+} transporters MagT1 [30] and SLC41A2 [31], but not via overexpression of TRPM6 WT alone [11].

Due to some conflicting data in literature, it still remains to be determined whether native TRPM6 homomers can form functional channels at the cell surface that are physiologically relevant, or if TRPM6/TRPM7 heteromers might represent the more common and functionally important configuration of these channels for cellular fate. In order to provide further insights into TRPM6 and TRPM7 function, we have carefully examined the biological effects of TRPM6 and TRPM7 co-expression in two different cellular systems, and demonstrate for the first time that TRPM6 phosphotransferase activity affects TRPM7 subcellular localization and cellular growth. We show that TRPM6 regulates TRPM7 trafficking, and that under hypomagnesic cell culture conditions, TRPM6 has an inhibitory effect on TRPM7-dependent cell growth.

2. Material and Methods

2.1. Cloning, cell culture and generation of cell lines overexpressing proteins of interest

A) The generation of HEK-293 T-Rex cells (Invitrogen) with transient or stable, doxycycline (dox)-inducible expression of human TRPM6 and TRPM7 wt and kinase dead or deletion mutants, as well as the cell culture conditions of these cells have been previously described [11]. In order to study the biological effects of Mg^{2+} deprivation, expression of proteins of interest in HEK-293 cells was induced with 1 μg/ml doxycycline for 24-48 hrs prior deprivation. After 12 hrs of induced protein expression regular HEK media was removed and replaced with customized, chemically defined, serum-free media (HyQ CCMI from Hyclone cat. SH30043.03) with different Mg^{2+} concentrations (0, 1 and 10 mM) and cells were cultured under these conditions for 18-24 hrs. Cell growth of TRPM6/7 co-expressing HEK cells was studied under the same culture conditions for 24 hrs, as indicated. Statistical analysis was performed to evaluate TRPM6 kinase dependent cell growth inhibition in both cellular systems (HEK-293 and DT40s). The standard error of the mean (SEM) was calculated for each group and a two-tailed t-test was performed on three separate experiments. Statistical significance of changes in TRPM7 expression in DT40 cells under varying Mg^{2+} concentrations was evaluated similarly.

B) The generation of TRPM7 deficient DT40 cells complemented with human TRPM7 WT (cWT M7) and a kinase dead mutant (cKR M7) has been described previously [10], as well as the co-expression of human TRPM7 WT and TRPM6 WT in $TRPM7^{-/-}$ DT40s [11]. The same published TRPM7 deficient cell clone complemented with hTRPM7 WT (cWT M7) was transfected with the same pcDNA5/TO construct encoding FLAG-tagged TRPM6 WT as the one used for transfection of HEK-293 cells. Two cell clones co-expressing TRPM7 and TRPM6 WT (cWT M7 + M6 WT), or TRPM7 WT and a TRPM6 kinase dead mutant (cWT M7 + M6 KR) with similar inducible TRPM6 protein expression levels as assessed by anti-FLAG immunoblotting were chosen for further analysis (fig. S1). The DT40 mutant cell lines described above and $TRPM7^{-/-}$ DT40 cells used as a negative control were cultured in chemically defined medium +10 mM $MgCl_2$ for normal cell maintenance and cell line generation. To perform imaging experiments and growth curves, serum- and Mg^{2+}-free medium was used as indicated (chemically defined HyQ CCM1 and customized Mg^{2+}-free HyQ CCM1 media were purchased from Hyclone and supplemented with 1% chicken serum (Sigma)).

2.2 In vitro phosphorylation assays of hTRPM6 WT, hTRPM7 WT and kinase deletion mutants of both channels

TRPM6 and TRPM7 WT and mutant channels were immunoprecipitated with anti-Flag or anti-HA coated beads. The beads were incubated 30 min at 32 °C in a total volume of 40 μl reaction buffer (50 mM Tris–HCl, 0.1 (v/v) β-mercaptoethanol, 10 nM Calyculin A, 2 or 10 mM MgAc, 1 mM $MnCl_2$, 0.5 mM $CaCl_2$, 100 μM Mg-ATP). Phosphorylation was analyzed following gel electrophoresis and by Anti-P-Serine immunoblotting. The pH was kept constant in all phosphorylation reactions at 7.2.

2.3. Immunoblotting

1×10^7 of HEK-293 cells expressing TRPM6 and TRPM7 were plated for *in vitro* phosphorylation experiment. To analyze protein expression levels of DT40 mutant cells, 0.1 to 0.5×10^7 DT40 mutant cells were plated and expression of the indicated molecules was induced by adding doxycycline to the growth media for 24–48 hours. HEK-293 or DT40 cells were lysed using standard protocols. Anti-Flag (Sigma) and anti-HA (Roche) immunoprecipitations were performed with cell lysates. Bound proteins from whole cell lysates or immunoprecipitated proteins were washed 3 times with lysis buffer, then separated by SDS/PAGE using 6% polyacrylamide gels, and transferred to a PVDF membrane. The membranes were analyzed by anti-Flag (Sigma), anti-HA (Roche) or a general anti-P-Ser antibody (from Cell Signaling, cat.# 2981) immunoblotting, as indicated. Blots were sometimes re-probed after stripping.

2.4. Immunocytochemistry protocol for DT40 and HEK-293 cells

$1\text{-}2 \times 10^4$ HEK-293 cells were plated on poly L-lysine coated 5-well slides (Tekdown). Cells were grown for 24 hours or until HEK cells were adhered to the slides and 60% confluent. Protein expression of interest was induced by adding 1 μg/ml doxycycline to the growth media. At the same time as induction, HEK cells were grown in customized, chemically defined, serum-free media (HyQ CCMI from Hyclone cat.# SH30043.03) with different Mg^{2+} concentrations (0 and 1 mM), and cultured under these conditions for 18-24 hours. In DT40 chicken B cells, protein expression was induced by the addition of 1μg/ml doxycycline to the growth medium for 20-24 hours. Growth media were replaced with the chemically defined media with varying concentrations of Mg^{2+} (0 and 1 mM) for 20-24 hours. DT40 cells were plated on the poly-L lysine coated, 5-well slides at a density of 100,000 cells/well and spun to adhere at 1000 RPM at 4° C for 10 minutes.

The cells were fixed and permeabilized in methanol at -20°C for at least 20 minutes. Nonspecific protein binding sites were blocked by a 30 minute preincubation in a blocking solution consisting of 10% v/v normal goat serum (NGS) in PBS. HA-tagged TRPM7 channels were labeled using a FITC conjugated, HA-tagged primary antibody (H7411, Sigma-Aldrich) diluted 1:1000 in 5% NGS/PBS. Slides were incubated with antibody either for 4 hours at room temperature or overnight at 4°C in a humid chamber. After washing with PBS (3 × 5 min) the slides were briefly rinsed with deionized H_2O, dried and coverslips were mounted using Vectashield antifade mounting medium (Vector, Burlingame, CA) that contained propidium iodide to label nuclei.

2.5. Image acquisition and Image quantification for DT40 and HEK-293 cells

Images of HEK and DT40 cells were obtained using a Nikon 100×/1.45 N oil immersion objective and a Nikon PCM-2000 laser scanning confocal microscope. Image collection was performed using SimplePCI software, v4.6 (Compix, Cranberry Township, PA). 0.5-μm stacks of images were acquired along the z axis of HEK-293 cells and DT40 B-cells. Each image was saved as a 16-bit file with a 1024 × 1024 pixel resolution where each square pixel was 0.12 μm in dimension and represented an area of 0.014 μm^2. Image quantification and processing was performed using the NIH Image J software (Rasband WS. *ImageJ*. 1997–2007. http://rsb.info.nih.gov/ij/). Background fluorescence for HA-FITC labeled cells was

calculated using TRPM7 KO or non-induced cells probed with the FITC conjugated mouse anti-HA antibody. Cells were classified as TRPM7 high if the HA-FITC staining intensity in the cytosol or membrane was three standard deviations above background. The “Z Project” function was used to compress Z-stacks of images by selecting for the maximum pixel intensity for each section. A straight line was drawn through DT40 cells and across the cytosolic regions of HEK-293 cells and the “Plot Profile” tool was used to create a histogram of pixel intensity along the line to measure intracellular distribution of TRPM7. Statistical analysis was performed using Graphpad Prism5 (Graphpad Software, San Diego, CA). One-way ANOVA and the bonferroni method were used to compare TRPM7 distribution across cell types and Mg^{2+} concentrations. Statistical significance of changes in TRPM7 expression in DT40 cells under varying Mg^{2+} concentrations was evaluated using a student t-test.

2.6. Cell surface labeling with biotin of HEK-293 cells

10^7 HEK-293 mutant cells were cultured and protein expression induced with doxycycline as described under 2.4. Intact cells were biotinylated with NHS-LC-biotin following the standard labeling protocol from Pierce (cat. 21335) at room temperature for 30 minutes, lysed and immunoprecipitated with NanoLink™ Streptavidin magnetic beads from Solulink (cat. M-1002-010), anti-Flag or anti-HA antibodies. Proteins were separated and transferred as described above under 2.3. The membranes were analyzed with horseradish peroxidase conjugated streptavidin (Sigma) – TRPM6 (Flag-tagged) and TRPM7 (HA-tagged) protein expression levels were analyzed via anti-HA or anti-Flag immunoblotting. The experiments have been performed at least three times independently. Cell surface immunoblots (fig. 3) were analyzed via densitometry using ImageJ [32], and statistically evaluated (student t-test).

3. Results

TRPM6 and TRPM7 are functionally non-redundant and appear to be co-expressed in a wide variety of cells. Although the formation of TRPM6/7 heteromers is well documented, the potential biological effects of this interaction remain mostly unknown. In the present study, we examined how TRPM6 and its kinase affect the cellular distribution and biological activity of TRPM7.

3.1. Serine cross-phosphorylation of TRPM7 by the kinase domain of its sister channel TRPM6 in HEK-293 cells

Both TRPM6 and TRPM7 contain a serine and threonine rich stretch of residues upstream of their intrinsic C-terminal kinase domains that is highly modified via phosphorylation [33]. The level of autophosphorylation of both channels improves substrate recognition and substrate phosphorylation of their kinases [33]. We previously found that TRPM6 and TRPM7 auto-phosphorylate threonine residues of their own channel, but that only TRPM6 cross-phosphorylates TRPM7 on threonine residues [11]. A detailed characterization of TRPM7 autophosphorylation has shown that 70% of phosphorylated TRPM7 C-terminal residues are serines, and 30% threonines [33]. Thus, we examined auto- and crossphosphorylation of serine residues of the channel kinases TRPM6 and TRPM7.

By co-expressing a full length channel with a kinase deletion mutant (Δkinase) in which the intrinsic kinase domain has been deleted, we were able to examine potential cross-phosphorylation of the Δkinase mutants by the full length channel [11]. We enriched the Flag-tagged TRPM6 and HA-tagged TRPM7 proteins by immunoprecipitation from HEK-293 cells for use in *in vitro* kinase assays. We detected phosphorylation by western blot using a general phosphoserine antibody. In HEK-293 cells expressing an intact TRPM7 wildtype channel and TRPM7 Δkinase we found that the TRPM7 kinase phosphorylates serine residues of the TRPM7 wildtype channel as well as of the TRPM7 Δkinase (fig. 1, top left panel, model bottom left panel), demonstrating that TRPM7 phosphorylates its own Ser residues in cis and in trans. In another series of phosphorylation experiments using HEK cells coexpressing TRPM6 WT and TRPM7 Δkinase mutants (top middle panel of fig. 1), we detected Ser phosphorylation of both the TRPM6 channel and the TRPM7 Δkinase mutant. These results indicate that TRPM6 can auto-phosphorylate Ser residues, as well as cross-phosphorylate TRPM7 Ser residues, in accordance with our previous observation that TRPM6 cross-phosphorylates TRPM7 on threonines. In contrast, when we co-expressed TRPM7 WT and TRPM6 Δkinase channels, we detected TRPM7 WT autophosphorylation but no TRPM6 Δkinase phosphorylation despite strong TRPM6 Δkinase protein expression (fig. 1, right top and bottom panel). We have previously demonstrated that the same cross-phophoryation pattern is seen using kinase dead mutants since TRPM7 is also not able to crossphosphorylate the TRPM6 K1804R mutant [11]. We are therefore confident that the ability of TRPM7 kinase to potentially crossphosphorylate TRPM6 is not impaired by the deletion of the entire TRPM6 kinase affecting the proper formation and conformation of TRPM6/7 heteromers.

Taken together, these results confirm that TRPM7 channels serves as a substrate of TRPM6 but not the reverse, further supporting the notion that despite their high homology, the kinases of TRPM6 and TRPM7 do not exhibit identical substrate specificities. It also brings up the question whether TRPM6-kinase activity can modulate TRPM7's biological activity. Changes in TRPM6/7 phosphorylation levels could influence channel heteromerization and localization, ion homeostasis regulation, as well as the regulation of TRPM6/7 kinase dependent intracellular signaling events, such as eEF2-kinase phosphorylation that influences protein translational rate and cell [19]. Therefore, in the following section we focused on whether TRPM6 kinase activity affects TRPM7 localization and TRPM7 dependent cell growth in intact cells.

3.2. Intracellular trafficking of TRPM7 is altered by TRPM6 kinase activity in HEK-293 cells

The above results confirm that TRPM6 and TRPM7 interact when co-expressed in HEK-293 cells. Multiple groups have demonstrated that TRPM7 is required for trafficking and formation of functional TRPM6-containing channels at the cell surface [11, 34]. In contrast, some studies reported measureable currents upon overexpression of TRPM6 alone, although it should be noted that native TRPM7 is present in the tested cells [1, 3, 35]. From our review of the literature, there are no studies examining the role of TRPM6 in TRPM7 trafficking. Multiple factors such as the formation of TRPM6 and TRPM7 heteromers, the phosphorylation status of the channels, and Mg^{2+} availability could affect intracellular trafficking of TRPM7.

We used immunocytochemistry to visualize the subcellular distribution of TRPM7 in HEK-293 cells under 1 and 0 mM Mg^{2+}. Changes in TRPM7 trafficking were measured by drawing 1-pixel histograms across the cell and classifying cells with steep peaks in intensity near the membrane of the cell as having increased peripheral trafficking. Cells that displayed little TRPM7 immunoreactivity near the periphery of the cell and shallow increases in intensity were deamed low peripheral TRPM7 trafficking. We found that HEK-293 cells overexpressing human TRPM7 WT alone, and grown in physiological (1 mM) levels of Mg^{2+} (fig. 2A-C), showed high levels of TRPM7 in the perinuclear regions of the cell that decreased in intensity towards the cell periphery with 34.0% +/- 3.1% of cells displaying increased peripheral trafficking of TRPM7 (fig. S2A). When cells overexpressing TRPM7 WT were grown in 0 mM Mg^{2+}, the percentage of cells displaying increased peripheral trafficking of TRPM7 rose to 58.8% +/- 4.1% ($p<0.01$, 1mM vs. 0 mM Mg^{2+}, figs. 2M-O, 5, and S2A). Furthermore, cells grown in 0 mM Mg^{2+} displayed signs of decreased health including cell rounding and a reduction in the extensive outgrowth detected in cells grown in 1 mM Mg^{2+} (fig. 2B versus fig. 2N).

The co-expression of TRPM7 WT with TRPM6 WT in HEK-293 cells (fig. 2D, E) produced extensive changes in both TRPM7 subcellular distribution and cellular morphology, under physiological and hypomagnesic conditions. TRPM7 WT + TRPM6 WT cells contained regions of high TRPM7 immunoreactivity termed clusters (fig. 2D-E), that produced the greatest levels of TRPM7 intensity while the rest of the cytoplasmic region contained low to undetectable regions of TRPM7. TRPM7 clusters were identified as regions of TRPM7 immunoreactivity greater than 0.5 μm in length in which TRPM7 intensity was above 200 on a scale of 0 to 250 (fig. 2F). Due to these bright clusters, images were collected using microscope settings low enough that the clusters did not saturate the entire image, but high enough to detect the low levels of TRPM7 near the periphery of the cell. TRPM7 clusters were detected in 60.7% +/- 8.0% (0 mM Mg^{2+}), and 50.8% +/- 9.2% (1 mM Mg^{2+}) of cells. In contrast, HEK-293 cells expressing TRPM7 WT alone produced very few clusters of TRPM7 in 1 mM Mg^{2+} (1.5% +/- 1.5% of cells, $P<0.01$) and in 0 mM Mg^{2+} (8.3% +/- 8.3%, $p<0.01$, fig. S2B.), indicating that cluster formation does not result from extracellular Mg^{2+} concentrations but from the presence of TRPM6 WT. Small peaks of TRPM7 immunoreactivity near the periphery of the cell were detectable in TRPM6 WT + TRPM7 WT HEK-293 cells in 46.1% +/- 4.1% of cells grown in 1 mM Mg^{2+} (fig. 2F, S2A), and in 50.8% +/- 9.2% of cells grown in 0 mM Mg^{2+} (fig. 2R, S2A). Indications of cellular toxicity (cell rounding and clumping, and nuclear breakdown) were evident in cells grown in both 0 and 1 mM Mg^{2+} (fig. 2E and 2Q), but more so in the cells starved of Mg^{2+}. Thus, the co-expression of TRPM6 and TRPM7 in the presence of an active TRPM6-kinase domain produces high-density clusters of TRPM7, elicits no further changes in trafficking of TRPM7 due to decreased Mg^{2} levels, and increases cellular toxicity.

We next examined whether the TRPM6 kinase affected TRPM7 trafficking and cellular health by overexpressing TRPM7 WT with TRPM6 KR mutants. The subcellular distribution of TRPM7 WT in HEK-293 cells co-expressing TRPM6 KR grown in 1 mM Mg^{2+} was similar to the TRPM7 distribution in HEK-293 cells overexpressing TRPM7 WT alone (figs. 2G-I, S2A). However, fewer TRPM7 WT + TRPM6 KR cells displayed peripheral trafficking of TRPM7 compared to TRPM7 WT cells when grown in 0 mM Mg^{2+}

(TRPM7 WT + TRPM6 KR: 38.4% +/- 3.8% vs. TRPM7 WT: 58.8% +/- 1.2% of cells with peripheral TRPM7 trafficking, P< 0.05, fig. 2S,T, fig. S2A). Potentially, the presence of the TRPM6 channel reduces Mg^{2+} dependent trafficking of TRPM7. In contrast to cells overexpressing TRPM7 WT and TRPM6 WT, cells that coexpressed the TRPM6 KR mutant produced significantly fewer clusters of TRPM7 (1mM Mg^{2+}: 4.0% +/- 4.8%, p< 0.01, 0 mM Mg^{2+}: 10.7% +/- 2.4%, p<0.001, fig. S2B), indicating that the TRPM6-kinase is involved in TRPM7 cluster formation. Surprisingly, the HEK-293 cells co-expressing TRPM7 WT and TRPM6 KR and grown in 0 mM Mg^{2+} appeared the healthiest of all TRPM6/7 ion channel overexpression combinations (fig. 2S,T). In the 0 mM Mg^{2+} growth conditions, the cells developed slightly more condensed outgrowth than the cells grown in 1 mM Mg^{2+}.

Our results indicate that a novel function of TRPM6 is to adjust the cellular distribution of TRPM7, which requires TRPM6's kinase activity. To further investigate the impact of TRPM6 on TRPM7's cellular localization, we next used a biochemical approach to analyze cell surface expression of TRPM7 in the same set of HEK-293 cells co-expressing TRPM7 with TRPM6 WT or kinase-dead.

3.3. TRPM6-kinase does not affect surface expression levels of co-expressed TRPM6/M7

Our immunocytochemistry (ICC) experiments showed that subcellular distribution of TRPM7 is affected by TRPM6 kinase activity. Due to the optical limits of confocal microscopy, we cannot determine whether TRPM7 is inserted into the membrane or merely targeted near the membrane using ICC. We thus performed surface biotinylation assays to measure TRPM7 surface expression in the presence of the TRPM6-kinase.

For each surface biotinylation assay, we labeled the cell surface of intact HEK-293 cells co-expressing either TRPM6 WT + TRPM7 WT, or TRPM6 KR + TRPM7 WT with biotin, and analyzed surface-expressed vs. total HA-TRPM7 or Flag-TRPM6 by immunoprecipitation and immunoblot. Our previously published TRPM6/7 surface biotinylation study in HEK-293 cells demonstrated that TRPM6 and TRPM7 have to associate in order for TRPM6 to be detected at the plasma membrane [11]. In the present study, we find that co-expressed TRPM6 and TRPM7 WT exhibit similar cell surface expression levels compared to TRPM7 co-expressed with the TRPM6 KR kinase dead mutant channel, both under physiological Mg^{2+} and hypomagnesic growth conditions (Fig. 3). Although there is a slight trend of lower surface expression of TRPM6/7 WT channels in comparison to TRPM6 KR/M7WT, this effect is not statistically significant. We thus conclude that TRPM6 and TRPM7 cell surface expression does not appear to be modulated by TRPM6 kinase.

Under conditions of Mg^{2+} deprivation, HEK-293 cells co-expressing TRPM6/7 WT show morphological signs of impaired cellular health (fig. 2P/Q). In the next section, we present results obtained in both, HEK 293 and DT40 cells, showing TRPM6-mediated growth impairment under suboptimal Mg^{2+} conditions, which is dependent upon an active TRPM6-kinase.

3.4. TRPM6 kinase activity inhibits TRPM7 dependent cell growth under hypomagnesic conditions

Inducible overexpression of the epitope-tagged TRPM6/7 channels in HEK-293 cells has proven reliable and convenient as it allows for the performance of studies that would not normally be feasible given the comparatively low levels of native expression of the channels and lack of reliable TRPM6/7-specific antibodies. Robust overexpression can however also be a source of artifacts. To further study the modulation of TRPM7 through TRPM6, we therefore opted to use a previously generated TRPM7$^{-/-}$ DT40 B-cell line (M7 KO) that also lacks endogenous TRPM6 (no RNA transcripts detectable [11]), and thus provides a clean slate to study exogenously expressed human TRPM6, TRPM7, and corresponding kinase dead mutants (fig. S1A). An additional advantage of the DT40 system is that the level of TRPM7 overexpression in the complemented TRPM7$^{-/-}$ DT40 cells is only 2-3 higher than native TRPM7 levels based on measured current intensities [20]. Thus the DT40 cell lines used diminish the potential for artifacts caused by strong overexpression. We previously described and characterized TRPM7$^{-/-}$ DT40 cells complemented with stably and inducibly overexpressed human TRPM7 WT (cWT M7), human TRPM7 K1648R kinase dead mutants (cKR M7), and co-expressed human TRPM6 and TRPM7 WT channels (cWT M7 + M6 WT) [10, 11]. For the present study, we have additionally generated TRPM7$^{-/-}$ DT40 cells complemented with stably and inducibly co-expressed TRPM7 WT and TRPM6 K1804R kinase dead mutants (cWT M7 + M6 KR, fig. S1).

We previously reported that TRPM7-deficient chicken DT40 B cells go into growth arrest and die under physiological Mg^{2+} growth conditions, but can be rescued by supplementation of the growth media with 10 mM Mg^{2+}, or by heterologous expression of human TRPM7 but not TRPM6 [10, 11]. Based on our results showing that TRPM6 crossphosphorylates TRPM7 on Thr and Ser residues, and that TRPM6 affects intracellular distribution and cell growth in HEK-293 cells, we used the complemented TRPM7$^{-/-}$ DT40 cell lines listed above to examine whether TRPM6 and TRPM7 co-expression might modulate TRPM7 dependent cell growth under varying Mg^{2+} conditions.

Under suboptimal Mg^{2+} concentrations (0.125 mM Mg^{2+}), TRPM7$^{-/-}$ DT40 and cWT M7 + M6 WT cells entered growth arrest after 2 days, whereas cWT M7 or cWT M7 + M6 KR cells still underwent cellular division under Mg^{2+} deprivation (fig. 4B). At 0.5 mM, the growth difference between these three cell lines (cWT M7, cWT M7 + M6 WT or cWT M7 + M6 KR) begins to become indistinguishable, and loses significance as the levels of Mg^{2+} are approaching optimal range (fig. 4 C). As already published in 2005, under physiological concentrations of 1 mM Mg^{2+} in the growth media, there were no observable differences between growth rates of the cWT M7 or cWT M7 + M6 mutant cells, whereas the TRPM7$^{-/-}$ DT40 growth rates decreased by half after five days (one control experiment replicating this finding is shown in fig. 4D).

Together, these results indicate that TRPM6 through its kinase activity has a detrimental, inhibitory effect on TRPM7 dependent cell growth, albeit only under hypomagnesic conditions. This observation parallels our cell growth results in HEK-293 cells (Fig. 4A).

3.5. The TRPM6 kinase domain promotes the clustered distribution of TRPM7 in DT40 B cells

The DT40 cell growth results led us to further question how the TRPM6 kinase domain might modulate TRPM7 in these cells. Given our observations in HEK-293 cells presented above, we hypothesized that the presence of the TRPM6 kinase domain, and possibly reduced availability of environmental Mg^{2+}, could also affect TRPM7 trafficking and subcellular distribution in DT40 cells. We examined TRPM7 protein expression and subcellular distribution in $TRPM7^{-/-}$ DT40 cells complemented with HA-tagged TRPM7 WT and co-expressing either TRPM6 WT or TRPM6 KR. Cells were starved for 24 hour periods before detection of TRPM7 using immunocytochemistry and confocal imaging. Immunostaining was controlled for using $TRPM7^{-/-}$ cells probed with rabbit anti-HA antibodies. Non-specific staining was not observed in the $TRPM7^{-/-}$ DT40 cells (fig. 5J-L). TRPM7 expression levels in DT40s vary cell to cell. In a subset of DT40 cells, TRPM7 immunoreactivity is not detectable using standard ICC measures. The cells with non-detectable TRPM7 are termed “TRPM7 low” while cells with detectable TRPM7 are termed “TRPM7 high.” We selected the most common cell type of TRPM7 high DT40 cells to analyze subcellular distribution of TRPM7, and selected representative images of TRPM7 cell expression patterns.

In cWT M7 DT40 cells grown in 1 mM Mg^{2+}, TRPM7 expression was diffuse throughout the cytoplasm, with high levels in the perinuclear region that decreased towards the membrane (fig. 5A-C). As with the TRPM7 WT HEK-293 cells, a subset of DT40 cWT M7 cells (47.6% +/- 2.4%, fig. S2C) displayed peripheral trafficking of TRPM7. When cWT M7 DT40 cells were starved of Mg^{2+} for 24 hours, a shift occurred in the subcellular localization of TRPM7 (fig. 5M-O). The line histogram from the one-pixel scan of cWT M7 cells (fig. 5O) depicts increased TRPM7 immunoreactivity in the periphery of the cell. The increased trafficking of TRPM7 to the periphery in cells grown in hypomagnesic conditions was detected in 65.7% +/- 2.1% of TRPM7 high cells, a significant increase over the 47.6% of TRPM7 high cells grown in 1 mM Mg^{2+} ($p<0.05$, fig. S2C). TRPM7 immunoreactivity in cWT M7 DT40 cells grown in 0 mM Mg^{2+} was uniform along both the plasma and nuclear membranes and expression levels were very low in the cytosol. These Mg^{2+}-mediated effects are similar to those seen for the HEK-293 TRPM7 WT expressing cells.

The presence of TRPM6-kinase altered the distribution of TRPM7 in DT40 cells co-expressing TRPM7 WT and TRPM6 WT when compared to cWT TRPM7 cells and the cell line co-expressing WT TRPM7 and the kinase-dead mutant TRPM6 KR. The cWT M7 + M6 WT DT40 cells displayed diffuse TRPM7 immunoreactivity throughout the cell (fig. 5D-F), with regions of clustered TRPM7 distribution reminiscent of the intracellular distribution pattern of TRPM7 in the corresponding HEK-293 cells co-expressing TRPM6/TRPM7 WT (fig. 2D-F). In the presence of the TRPM6-kinase, trafficking of TRPM7 to the periphery of the cell does not increase under hypomagnesic conditions as it does in cWT M7 DT40 cells (fig. S2 C), but results in an increase in overall TRPM7 expression (fig. S2D, 35.4% +/- 1.2% vs. 7.5% +/- 0.8%, $P<0.001$). Further supporting the role of the TRPM6-kinase regulating subcellular distribution of TRPM7, we found that cWT M7 + M6 KR cells had the lowest level of immunoreactivity (fig. 5G-I) and TRPM7 distribution was very

diffuse, with only 31.0% +/- 6.0% of cell displaying measurable immunoreactivity near the periphery of the cell (fig. S2C) and no change in TRPM7 trafficking was measured between cWT M7 + M6 KR DT40 cells grown in 1 mM or 0 mM Mg^{2+}.

In summary, we find that similarly to HEK-293 cells, DT40 cells expressing TRPM7 WT + TRPM6 WT displayed altered subcellular localization of TRPM7 as compared to cells expressing TRPM7 alone, or expressing TRPM7 with TRPM6 KR. The changes seen in DT40 cell lines were similar to those observed in the corresponding HEK cell lines, although not as pronounced, possibly because the level of overexpression is substantially lower in the DT40 cells. Both sets of results demonstrate that the presence of a functional TRPM6 kinase domain affects TRPM7 trafficking and protein expression in a Mg^{2+} dependent manner. This novel mechanism of TRPM7-regulation could alter Mg^{2+}-homeostasis, providing a potential explanation for the growth inhibition phenotype we see in the cWT M7 + M6 WT DT40 cells (fig. 4).

4. Discussion

The discovery and primary characterization of multiple Mg^{2+} transporters (Acdp2, MagT1, Mrs2, Paracellin-1, SLC41A1, SLC41A2, TRPM6 and TRPM7 (reviewed in [6, 36]) in eukaryotes over the last decade has contributed to a better understanding about molecular mechanisms of Mg^{2+} homeostasis regulation. These discoveries have improved our knowledge about how the movement of Mg^{2+} across cell membranes is regulated, and how Mg^{2+} might play a role in signaling as a second messenger, influencing numerous cellular processes. Furthermore, these studies highlight the potential contribution of Mg^{2+} to the development of various human diseases. Functionally defective Mg^{2+} transporters have been documented and shown to cause severe pathologies. Patients with deficiencies in TRPM6 develop Hypomagnesemia with Secondary Hypocalcemia (HSH), an autosomal recessive disorder leading to muscle spasms and tetany that can be treated with life-long Mg^{2+}-supplementation [4, 5]. Mutations in the Mg^{2+} transporter MagT1 are linked to a human disease named XMEN (X-linked immunodeficiency with Magnesium defect, chronic Epstein Barr virus infections and Neoplasia) [37, 38], and the T1482I genetic polymorphism in TRPM7 has been associated with neurodegenerative disorders of a subpopulation of patients on the island of Guam [39].

In the present study, we examined the impact of TRPM6 on TRPM7's biological activity under normomagnesic and hypomagnesic conditions. Recent studies indicating a broader cellular expression pattern of TRPM6 than originally assumed underscore the need to understand the physiological significance of TRPM7 and TRPM6 heteromeric channels. The presence of TRPM6 in cells expressing TRPM7 raises multiple questions, including how TRPM6 channel subunits affect TRPM7 channel function in TRPM6/7 heteromers, and how TRPM7 phosphorylation via the TRPM6 kinase influences TRPM7 function.

Previous research examining TRPM6 surface trafficking produced conflicting results. Two groups detected measureable TRPM6 currents at the cell membrane upon TRPM6 overexpression [1, 3, 35], whereas Chubanov and colleagues only saw changes in TRPM6-mediated current amplification upon TRPM7 co-expression, and observed that TRPM6

plasma membrane expression was found solely in co-localization with TRPM7 [34]. These latter findings are in agreement with our previous cell surface biotinylation studies, which failed to show detectable TRPM6 expression at the cell surface in the absence of TRPM7 channels [11]. In this same study we also reported the heteromultimerization between TRPM6 and TRPM7, as well as TRPM6 kinase mediated phosphorylation of TRPM7 on threonines. Additionally, we described the inhibition of cell growth of TRPM7$^{-/-}$ cells co-expressing wildtype TRPM6 and TRPM7, however only under hypomagnesic growth conditions. In a very recently published pharmacological study in collaboration with Dr. Fleig's group, TRPM6 phosphotransferase activity was found to play an important role in regulating MgATP sensitivity of TRPM6/7 heteromeric ion channels [40], supporting the idea that TRPM6 kinase activity modulates TRPM7 functionality.

The formation of heteromultimers plays in general an important role in TRP channel biology. Heteromultimerization can alter the ion permeability, as well as modes of channel regulation and cellular distribution when compared to the corresponding homomers (reviewed in [41]). Several studies showed the assembly of closely related TRPC subunits (TRPC1/4/5 and TRPC3/6/7), and how heteromers formation affects the function and biophysical properties of the channels [42-44]. A different study demonstrated a direct link between the TRPP1/TRPP2 interaction and the translocation of TRPP2 channels from intracellular compartments to the plasma membrane [45]. The same research group also reported that TRPML3 channels are expressed in the membrane of lysosomes instead of the endoplasmic reticulum when forming heteromultimers with TRPML1 or TRPML2 [46]. Mutations in TRPML1 are associated with the autosomal recessive lysosomal storage disorder Mucolipidosis type IV, and disrupted TRPML1/2 lysosome localization prevents TRPML3 trafficking to the lysosomes as well. These studies emphasize the importance of TRP channel heteromultimerization for their subcellular trafficking, and thus for their function. Compromised Mg^{2+} homeostasis regulation in patients could therefore be caused by impaired TRPM6/7 multimerization and localization.

While TRPM6 and TRPM7 are close homologues, the two channel-kinases show differences in their substrate specificity. Our previous cross-phosphorylation studies between wildtype and kinase-deleted TRPM6 and TRPM7 channels focused on threonine phosphorylations. More than 30 TRPM7 serine phosphorylation sites have been described in the TRPM7 C-terminus alone [33]. In the present study, we thus expended our TRPM6 and TRPM7 cross-phosphorylation studies to investigate serine phosphorylation. We determined that as expected both channels are able to autophosphorylate serines in their own C-terminus, but whereas TRPM6 cross-phosphorylates TRPM7, TRPM7 does not phosphorylate serine residues in TRPM6. These results replicate our previous analyses of the Thr-phosphorylation pattern, and confirm that TRPM7 and TRPM6 do not share identical substrate kinase relationships, suggesting that these channels might differentially influence each other's activity.

Of particular interest in the context of the potential biological effect of TRPM7 phosphorylation are two recent studies showing a direct link between a human polymorphism resulting in the exchange of threonine 1482 to isoleucine, and two different human diseases. Hermosura and colleagues identified the TRPM7 T1482I variant in a subset

of patients who lived in an environment deficient in Ca^{2+} and Mg^{2+}, and presented with Guamanian amyotrophic lateral sclerosis and parkinsonism dementia [39]. TRPM7 T1482I channels have an increased sensitivity towards intracellular Mg^{2+} with an intact TRPM7 kinase activity, but decreased TRPM7 threonine autophosphorylation [39]. The TRPM7 1482 threonine residue lies in the C-terminal Ser/Thr rich linker between the TRPM7 kinase domain and its upstream domain, and has been described as a potential phosphorylation site via mass spectrometry [33]. Dai and colleagues recently showed a direct correlation between Ca^{2+} and Mg^{2+} intake, the TRPM7 T1482I polymorphism, and the risk of colorectal cancer development. These investigators report that the TRPM7 1482 polymorphism appears to be common in human populations, and is associated with a higher risk of adenomatous and hyperplastic polyp occurrence [47]. Given its high expression in the colon, it is possible that TRPM6 kinase activity might play a role in modulating TRPM7 biological function by adjusting its Mg^{2+} sensitivity via phosphorylation, although future studies will need to address this question.

In the present study, we show for the first time a connection between phosphotransferase activity, trafficking, and intracellular localization of the TRPM6/7 channel-kinases. Although the effect varies depending on the cell type, level of channel expression, and Mg^{2+} availability, we observe similar trends of intracellular redistribution of TRPM7 when TRPM6 WT is co-expressed. In the strong TRPM6/7 overexpressing HEK-293 cell lines and in the complemented DT40 B cells in which TRPM7 overexpression is only 2-3 times above native levels, TRPM7-specific staining changes from a diffuse to a clustered distribution upon TRPM6 WT co-expression. This phenomenon is absent when a kinase-dead version of TRPM6 is co-expressed, strongly suggesting that TRPM6 mediated cross-phosphorylation of TRPM7 plays a role in its intracellular relocalization. But only when expressed alone did TRPM7 trafficking to the periphery increase in a Mg^{2+}-dependent manner. In the presence of TRPM6 WT or KR, this phenotype was abolished in both cellular systems analyzed.

The delivery and insertion of ion channels into the plasma membrane is a regulated process that contributes to the cellular regulation of ion channel activity [48-50]. We therefore performed cell surface labeling experiments of intact HEK-293 cells with biotin to investigate the possibility that TRPM6/M7 multimerization influences surface expression of the channels. We found that under both, physiological and suboptimal Mg^{2+} growth conditions, co-expression of TRPM6 and TRPM7 does not appear to significantly impact levels of the channels at the plasma membrane (fig. 3). However, the TRPM6-kinase dependent alterations in intracellular TRPM7 localization we observed (figs. 2 and 5) might for example affect TRPM6/7 mediated signaling. This could provide some explanation for our findings that under suboptimal Mg^{2+} conditions, the DT40 $TRPM7^{-/-}$ complementation cell lines and HEK-293 cells co-expressing TRPM7 WT and TRPM6 KR kinase dead mutant channels have a growth advantage in comparison to the corresponding TRM6/7 WT co-expressing cell lines.

In HEK-293 cells, we found that both Mg^{2+} deprivation and TRPM6/TRPM7 co-expression resulted in changes in cellular morphology, decreased cellular adherence, and growth inhibition. HEK-293 cells overexpressing TRPM7 have been described to swell, detach, and begin to die 24 hours post induction of overexpression [51]. In contrast, knock down of

TRPM7 in HEK-293 cells caused increased cellular adherence [52]. In a follow-up study, Su and colleagues determined TRPM7 overexpression initiated a stress response brought on by the constitutive permeation of both Ca^{2+} and Mg^{2+} into cells [53], which included increases in reactive oxygen species and nitric oxide, resulting in the activation of p38 MAPK and c-Jun N-terminal kinase (JNK).

The formation of TRPM6/TRPM7 heteromers could additionally regulate cell morphology via phosphorylation of the cytoskeletal element myosin IIA. High levels of autophosphorylation of the Ser/Thr-rich domain N-terminal to the kinase domain of TRPM6 and TRPM7 increases the channel-kinase phosphorylation of Myosin IIA [18, 33], leading to Ca^{2+} dependent association of TRPM7 with myosin IIA, phosphorylation and dissociation of myosin filaments, and ultimately cytoskeletal remodeling [18]. As we found that TRPM6 cross-phosphorylates TRPM7 in this Ser/Thr rich domain, it is possible that increased phosphorylation of TRPM7 in TRPM6/TRPM7 heteromers, might lead to elevated phosphorylation of myosin IIA. The reduction in rounding and detachment of HEK-293 cells overexpressing simultaneously TRPM7 WT and kinase-dead TRPM6 KR further supports this idea.

When we analyzed cellular growth of $TRPM7^{-/-}$ DT40 cells complemented with TRPM7 and co-expressing either TRPM6 WT or KR mutant we found that TRPM6 kinase activity is required for the inhibition of TRPM7 dependent cellular growth. Similarly to the trafficking phenotype described above, the presence of a functional TRPM6 kinase inhibits DT40 cells growth, but only under hypomagnesic conditions. This also correlates with the poor health of HEK-293 cells that overexpressed both WT forms of TRPM6 and TRPM7. Thus, the formation of TRPM6/TRPM7 heteromers influences the cellular localization patterns of each channel, and inhibits TRPM7 dependent cellular growth under hypomagnesic conditions, however only when TRPM6 phosphotransferase activity is intact. The change in TRPM7 cellular distribution in the presence of TRPM6 could affect Mg^{2+} homeostasis, as well as downstream signaling events via the phosphorylation of known TRPM6/TRPM7 substrates such as annexin, eEF2-k, PLC γ-2 or cytoskeleton components [17-20].

Alterations in extracellular Mg^{2+} concentrations affected not only the TRPM7 phenotypes in the presence of the WT TRPM6 channel-kinase, but influenced cellular growth and TRPM7 distribution in all cells. The increase in TRPM7 trafficking to the periphery of cells deprived of Mg^{2+} could represent a survival mechanism to increase intracellular concentrations of this essential nutrient. DT40 cells expressing TRPM7 displayed reduced rates of cellular growth under hypomagnesic conditions (0 mM Mg^{2+}) while TRPM7 deficient DT40 cells had reduced growth rates under physiological and complete growth inhibition under hypomagnesic conditions. If Mg^{2+} levels are used as an indicator of metabolic health in a cell, increasing or redistributing TRPM7 protein levels could be a means to increase Mg^{2+} concentrations to better cellular growth and survival. Our finding that TRPM6 KR kinase dead mutants did not inhibit cell growth, nor greatly alter TRPM7 trafficking, suggests that TRPM6 kinase activity is involved in modulating TRPM7 trafficking, TRPM7 phosphotransferase activity, or TRPM7 Mg^{2+}-transport function, all of which will need to be clarified in future studies.

5. Conclusions

Our study shows that TRPM6's kinase activity modulates TRPM7 subcellular distribution and affects cell growth under hypomagnesic growth conditions, implying that both channel-kinases are in their own way important components of ion homeostasis regulation and pivotal signaling modules influencing each other's biological activity as well as intracellular signaling events. These findings confirm that although the channel kinases TRPM6 and TRPM7 are both environmental Mg^{2+} sensors and regulators of Mg^{2+}-homeostasis, they do not overlap functionally, as also shown by the phenotype of mice lacking TRPM6 or TRPM7, or of TRPM6-deficient patients.

Supplementary Material

Refer to Web version on PubMed Central for supplementary material.

Acknowledgments

This paper was supported by NIH training grant 5 T32 A1007405 (NIAID) to K.B., by NIH grant 5R01GM068801 (NIGMS) to A.L.P. and by NIH grants 5R21AI088421 (NIAID) and 5R01GM090123 (NIGMS & Office of Dietary Supplements) to C.S. We thank Dr. Fabienne Gally for carefully reviewing the manuscript.

References

1. Voets T, et al. TRPM6 forms the Mg2+ influx channel involved in intestinal and renal Mg2+ absorption. J Biol Chem. 2004; 279(1):19–25. [PubMed: 14576148]
2. Jiang J, Li M, Yue L. Potentiation of TRPM7 inward currents by protons. J Gen Physiol. 2005; 126(2):137–50. [PubMed: 16009728]
3. Li M, Jiang J, Yue L. Functional characterization of homo- and heteromeric channel kinases TRPM6 and TRPM7. J Gen Physiol. 2006; 127(5):525–37. [PubMed: 16636202]
4. Schlingmann KP, et al. Hypomagnesemia with secondary hypocalcemia is caused by mutations in TRPM6, a new member of the TRPM gene family. Nat Genet. 2002; 31(2):166–70. [PubMed: 12032568]
5. Walder RY, et al. Mutation of TRPM6 causes familial hypomagnesemia with secondary hypocalcemia. Nat Genet. 2002; 31(2):171–4. [PubMed: 12032570]
6. Brandao K, et al. The role of Mg2+ in immune cells. Immunol Res. 55(1-3):261–9. [PubMed: 22990458]
7. Jin J, et al. Deletion of Trpm7 disrupts embryonic development and thymopoiesis without altering Mg2+ homeostasis. Science. 2008; 322(5902):756–60. [PubMed: 18974357]
8. Ryazanova LV, et al. TRPM7 is essential for Mg(2+) homeostasis in mammals. Nat Commun. 2010; 1:109. [PubMed: 21045827]
9. Woudenberg-Vrenken TE, et al. Transient receptor potential melastatin 6 knockout mice are lethal whereas heterozygous deletion results in mild hypomagnesemia. Nephron Physiol. 2011; 117(2): 11–9.
10. Schmitz C, et al. Regulation of vertebrate cellular Mg2+ homeostasis by TRPM7. Cell. 2003; 114(2):191–200. [PubMed: 12887921]
11. Schmitz C, et al. The channel kinases TRPM6 and TRPM7 are functionally nonredundant. J Biol Chem. 2005; 280(45):37763–71. [PubMed: 16150690]
12. Ryazanova LV, et al. Characterization of the protein kinase activity of TRPM7/ChaK1, a protein kinase fused to the transient receptor potential ion channel. J Biol Chem. 2004; 279(5):3708–16. [PubMed: 14594813]
13. Yamaguchi H, et al. Crystal structure of the atypical protein kinase domain of a TRP channel with phosphotransferase activity. Mol Cell. 2001; 7(5):1047–57. [PubMed: 11389851]

14. Runnels LW. TRPM6 and TRPM7: A Mul-TRP-PLIK-cation of channel functions. Curr Pharm Biotechnol. 12(1):42–53. [PubMed: 20932259]

15. Matsushita M, et al. Channel function is dissociated from the intrinsic kinase activity and autophosphorylation of TRPM7/ChaK1. J Biol Chem. 2005; 280(21):20793–803. [PubMed: 15781465]

16. Crawley SW, Cote GP. Identification of dimer interactions required for the catalytic activity of the TRPM7 alpha-kinase domain. Biochem J. 2009; 420(1):115–22. [PubMed: 19228120]

17. Dorovkov MV, Ryazanov AG. Phosphorylation of annexin I by TRPM7 channel-kinase. J Biol Chem. 2004; 279(49):50643–6. [PubMed: 15485879]

18. Clark K, et al. TRPM7, a novel regulator of actomyosin contractility and cell adhesion. Embo J. 2006; 25(2):290–301. [PubMed: 16407977]

19. Perraud AL, et al. The channel-kinase TRPM7 regulates phosphorylation of the translational factor eEF2 via eEF2-k. Cell Signal. 2011; 23(3):586–93. [PubMed: 21112387]

20. Deason-Towne F, Perraud AL, Schmitz C. Identification of Ser/Thr phosphorylation sites in the C2-domain of phospholipase C gamma2 (PLCgamma2) using TRPM7-kinase. Cell Signal. 2012; 24(11):2070–2075. [PubMed: 22759789]

21. Sahni J, Scharenberg AM. TRPM7 ion channels are required for sustained phosphoinositide 3-kinase signaling in lymphocytes. Cell Metab. 2008; 8(1):84–93. [PubMed: 18590694]

22. Wei C, et al. Calcium flickers steer cell migration. Nature. 2009; 7231; 457:901–5. [PubMed: 19118385]

23. Asrar S, Aarts M. TRPM7, the cytoskeleton and neuronal death. Channels (Austin). 7(1):6–16. [PubMed: 23247582]

24. Middelbeek J, et al. The alpha-kinase family: an exceptional branch on the protein kinase tree. Cell Mol Life Sci. 67(6):875–90. [PubMed: 20012461]

25. Wolf FI, Trapani V. Magnesium and its transporters in cancer: a novel paradigm in tumour development. Clin Sci (Lond). 123(7):417–27. [PubMed: 22671428]

26. Middelbeek J, et al. TRPM7 is required for breast tumor cell metastasis. Cancer Res. 72(16):4250–61. [PubMed: 22871386]

27. Walder RY, et al. Mice defective in Trpm6 show embryonic mortality and neural tube defects. Hum Mol Genet. 2009; 18(22):4367–75. [PubMed: 19692351]

28. Feske S, Skolnik EY, Prakriya M. Ion channels and transporters in lymphocyte function and immunity. Nat Rev Immunol. 12(7):532–47. [PubMed: 22699833]

29. Desai BN, et al. Cleavage of TRPM7 releases the kinase domain from the ion channel and regulates its participation in Fas-induced apoptosis. Dev Cell. 22(6):1149–62. [PubMed: 22698280]

30. Deason-Towne F, Perraud AL, Schmitz C. The Mg(2+) transporter MagT1 partially rescues cell growth and Mg(2+) uptake in cells lacking the channel-kinase TRPM7. FEBS Lett. 2011; 585(14): 2275–8. [PubMed: 21627970]

31. Sahni J, Nelson B, Scharenberg AM. SLC41A2 encodes a plasma-membrane Mg2+ transporter. Biochem J. 2007; 401(2):505–13. [PubMed: 16984228]

32. Schneider CA, Rasband WS, Eliceiri KW. NIH Image to ImageJ: 25 years of image analysis. Nat Methods. 9(7):671–5. [PubMed: 22930834]

33. Clark K, et al. Massive autophosphorylation of the Ser/Thr-rich domain controls protein kinase activity of TRPM6 and TRPM7. PLoS One. 2008; 3(3):e1876. [PubMed: 18365021]

34. Chubanov V, et al. Disruption of TRPM6/TRPM7 complex formation by a mutation in the TRPM6 gene causes hypomagnesemia with secondary hypocalcemia. Proc Natl Acad Sci U S A. 2004; 101(9):2894–9. [PubMed: 14976260]

35. Thebault S, et al. EGF increases TRPM6 activity and surface expression. J Am Soc Nephrol. 2009; 20(1):78–85. [PubMed: 19073827]

36. Quamme GA. Molecular identification of ancient and modern mammalian magnesium transporters. Am J Physiol Cell Physiol. 2010; 298(3):C407–29. [PubMed: 19940067]

7. Li FY, et al. Second messenger role for Mg2+ revealed by human T-cell immunodeficiency. Nature. 2011; 475(7357):471–6. [PubMed: 21796205]

38. Chaigne-Delalande B, et al. Mg2+ regulates cytotoxic functions of NK and CD8 T cells in chronic EBV infection through NKG2D. Science. 341(6142):186–91. [PubMed: 23846901]
39. Hermosura MC, et al. A TRPM7 variant shows altered sensitivity to magnesium that may contribute to the pathogenesis of two Guamanian neurodegenerative disorders. Proc Natl Acad Sci U S A. 2005; 102(32):11510–5. [PubMed: 16051700]
40. Zhang Z, et al. The TRPM6 kinase domain determines the Mg.ATP sensitivity of TRPM7/M6 heteromeric ion channels. J Biol Chem. 289(8):5217–27. [PubMed: 24385424]
41. Venkatachalam K, Montell C. TRP channels. Annu Rev Biochem. 2007; 76:387–417. [PubMed: 17579562]
42. Strubing C, et al. TRPC1 and TRPC5 form a novel cation channel in mammalian brain. Neuron. 2001; 29(3):645–55. [PubMed: 11301024]
43. Hofmann T, et al. Subunit composition of mammalian transient receptor potential channels in living cells. Proc Natl Acad Sci U S A. 2002; 99(11):7461–6. [PubMed: 12032305]
44. Mace KE, et al. TRUSS, TNF-R1, and TRPC ion channels synergistically reverse endoplasmic reticulum Ca2+ storage reduction in response to m1 muscarinic acetylcholine receptor signaling. J Cell Physiol. 225(2):444–53. [PubMed: 20458742]
45. Montell C. The TRP superfamily of cation channels. Sci STKE. 2005; 2005(272):re3. [PubMed: 15728426]
46. Venkatachalam K, Hofmann T, Montell C. Lysosomal localization of TRPML3 depends on TRPML2 and the mucolipidosis-associated protein TRPML1. J Biol Chem. 2006; 281(25):17517–27. [PubMed: 16606612]
47. Dai Q, et al. The relation of magnesium and calcium intakes and a genetic polymorphism in the magnesium transporter to colorectal neoplasia risk. Am J Clin Nutr. 2007; 86(3):743–51. [PubMed: 17823441]
48. Beech DJ. Integration of transient receptor potential canonical channels with lipids. Acta Physiol (Oxf). 204(2):227–37. [PubMed: 21624095]
49. Toro CA, Arias LA, Brauchi S. Sub-cellular distribution and translocation of TRP channels. Curr Pharm Biotechnol. 12(1):12–23. [PubMed: 20932262]
50. Cayouette S, Boulay G. Intracellular trafficking of TRP channels. Cell Calcium. 2007; 42(2):225–32. [PubMed: 17368756]
51. Nadler MJ, et al. LTRPC7 is a Mg.ATP-regulated divalent cation channel required for cell viability. Nature. 2001; 411(6837):590–5. [PubMed: 11385574]
52. Su LT, et al. TRPM7 regulates cell adhesion by controlling the calcium-dependent protease calpain. J Biol Chem. 2006; 281(16):1260–70.
53. Su LT, et al. TRPM7 activates m-calpain by stress-dependent stimulation of p38 MAPK and c-Jun N-terminal kinase. J Mol Biol. 396(4):858–69. [PubMed: 20070945]

Abbrevations

TRPM6 and TRPM7	Transient receptor potential cation channel, subfamily Melastatin, member 6 and 7
HSH	Hypomagnesemia with Secondary Hypocalcemia
XMEN	X-linked immunodeficiency with Magnesium defect, chronic Epstein Barr virus infections and Neoplasia

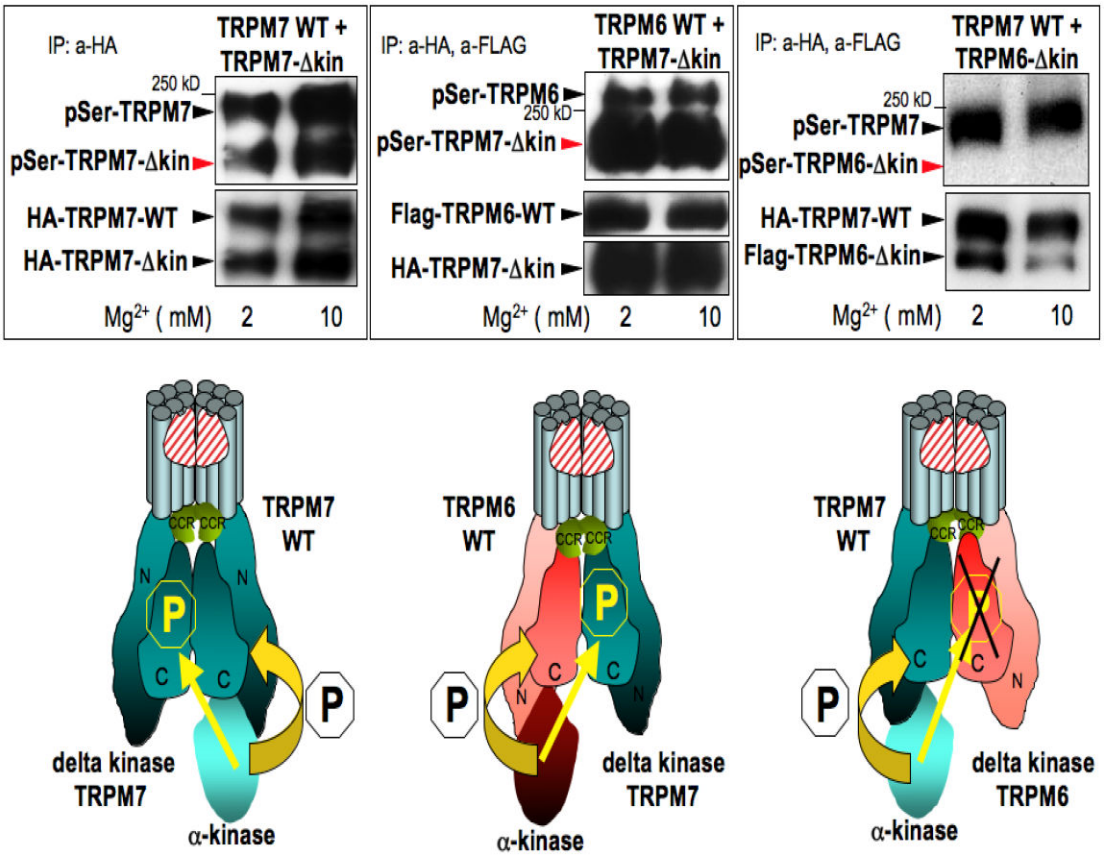

Figure 1. The channel-kinase TRPM6 phosphorylates serine residues of associated TRPM7 but not vice versa

Human HA-tagged TRPM7 WT, human HA-tagged TRPM7 delta kinase (TRPM7-Δkin), human Flag-tagged TRPM6 WT, and human Flag-tagged TRPM6 delta kinase (TRPM6-Δkin) have been cloned, stably transfected and inducibly co-expressed in HEK-293 cells as indicated, see methods section and reference [11] for further details.

In vitro phosphorylation reactions have been performed after HA and/or Flag immunoprecipiations under two different Mg^{2+} concentrations (2 and 10 mM) with 100 μM MgATP [11]. Phosphorylation of these proteins was subsequently analyzed after gel electrophoresis and immunoblotting with a general anti phospho serine antibody. Protein expression levels were verified after stripping of the membrane via reprobing with anti FLAG or anti HA antibodies.

A. Left panel: TRPM7 kinase crossphosphorylates TRPM7 delta kinase channels in vitro upon TRPM7 WT and TRPM7 delta kinase co-expression.

Middle panel: TRPM6 kinase crossphosphorylates TRPM7 delta kinase channels in vitro upon TRPM6 WT and TRPM7 delta kinase co-expression.

Right panel: TRPM7 kinase does not crossphosphorylate TRPM6 delta kinase channels in vitro upon TRPM7 WT and TRPM6 delta kinase co-expression.

These data are representative of three separate experiments.

B: Based on our results, model showing how TRPM6 and TRPM7 form heteromers and crossphosphorylate each other. Note: TRPM6 and TRPM7 have to tetramerize in order to build a functional ion channel pore.

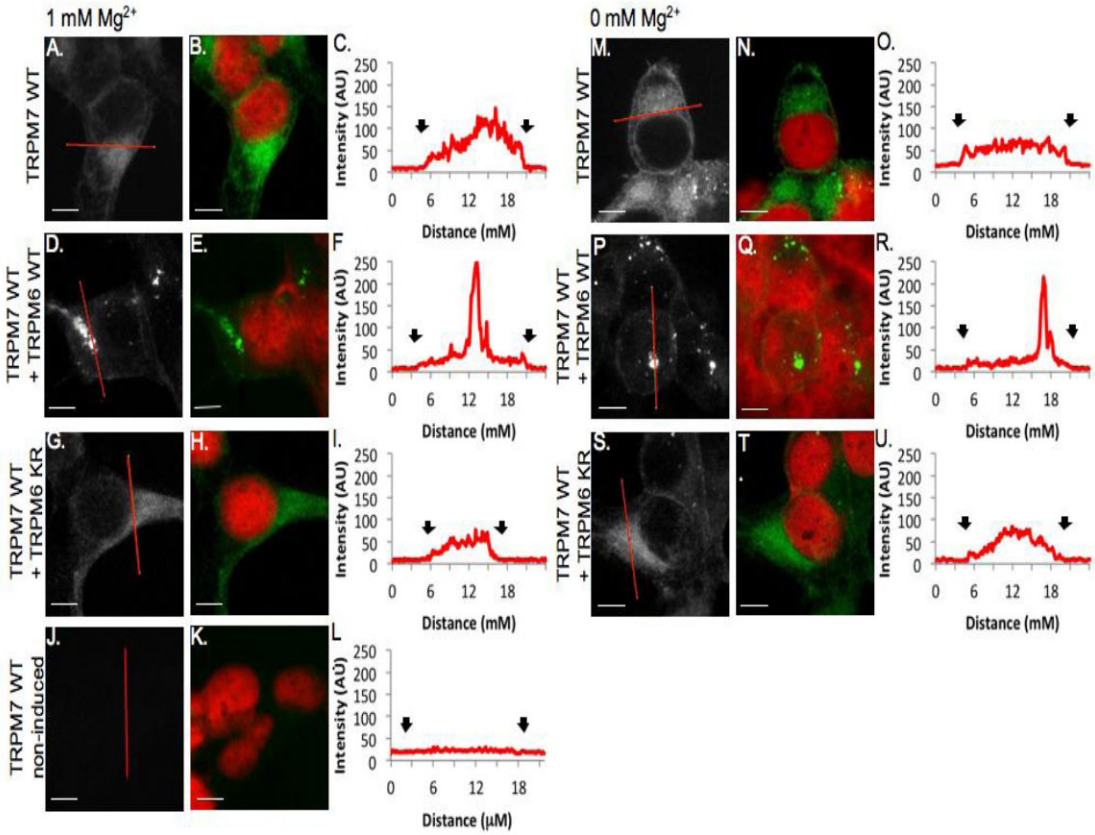

Figure 2. TRPM7 cellular trafficking is regulated by TRPM6 kinase activity in HEK-293 cells

100x confocal images of HA-tagged TRPM7 channels visualized with HA-FITC antibody (grey scale, green) and nuclei visualized with propidium iodide (red). Scale bars = 5 μM.

A-I. HEK cells overexpressing TRPM7 and TRPM6 channels grown with physiological Mg^{2+} levels (1 mM). Little immunoreactivity is detected in non-induced HEK mutant cells (J-L).

M-U. HEK-293 cells overexpressing TRPM7 and TRPM6 channels grown with 0mM Mg^{2+}. (C,F,I,L,O,R,U). Representative histograms of pixel intensity across cytoplasmic sections of cells (red line in A,D,G,J,M,P,S). Black arrows indicate membrane borders of the cell.

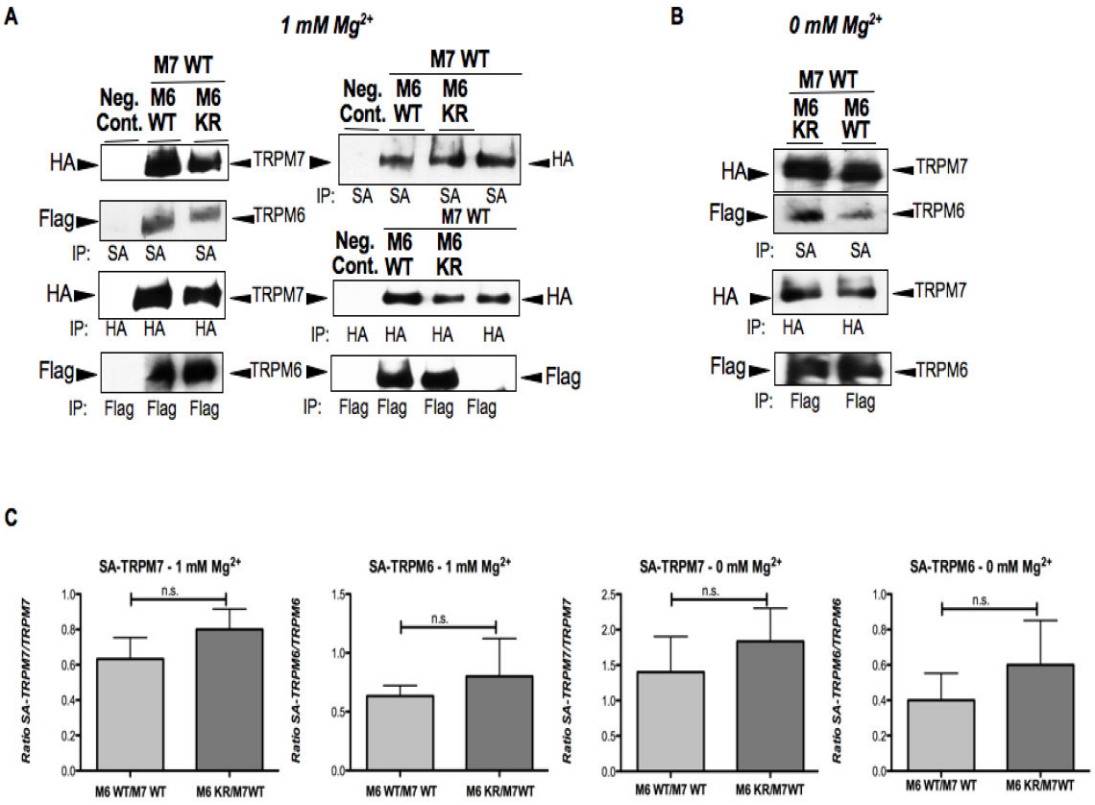

Figure 3. TRPM6 kinase activity does not affect TRPM7 expression levels at the plasma membrane under normal or hypogmagnesic growth conditions in HEK-293 cells

Analysis of biotin cell surface labeled cells (co-)expressing TRPM6/7 WT or TRPM6 kinase dead mutant (M6 KR) channels. Cells were cultured under 1 or 0 mM Mg^{2+}. The channels were subsequently immunoprecipitated with streptavidin magnetic beads (SA) and analyzed by immunoblotting with HA- or Flag-horseradish peroxidase. TRPM6 (Flag tagged) and TRPM7 (HA tagged) protein expression levels were determined by HA- and Flag-immunoblotting accordingly.

Fig. 3A, at 1 mM Mg^{2+}, left panel shows TRPM6 and TRPM7 at the plasma membrane, right panel shows additionally TRPM7 alone. Fig. 3B, at 0 mM Mg^{2+}, shows TRPM6/7 surface expression, w or w/o TRPM6's active kinase. Fig. 3C: Densitometric analysis of three independent experiments using ImageJ of TRPM6/7 surface expression levels as shown in fig. 3A/B (ratio of SA-TRPM7 or SA-TRPM6 divided by corresponding total protein amount). (n.s. not significant, student t-test).

A

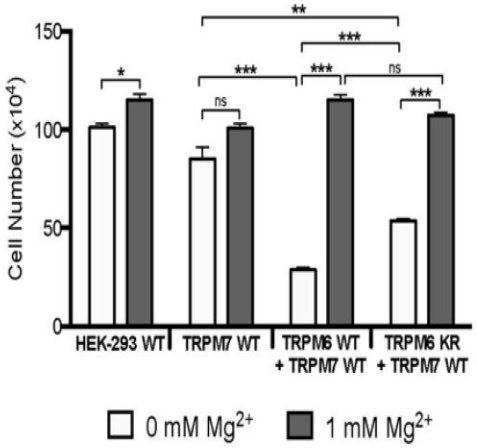

B

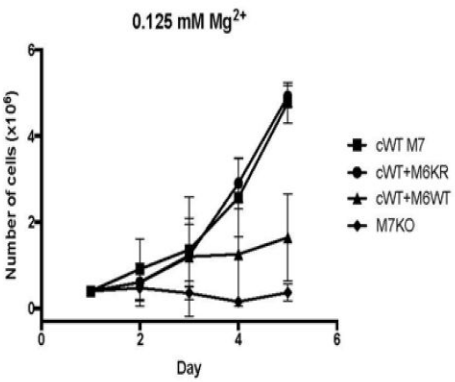

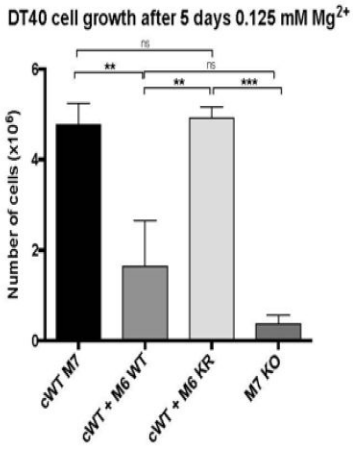

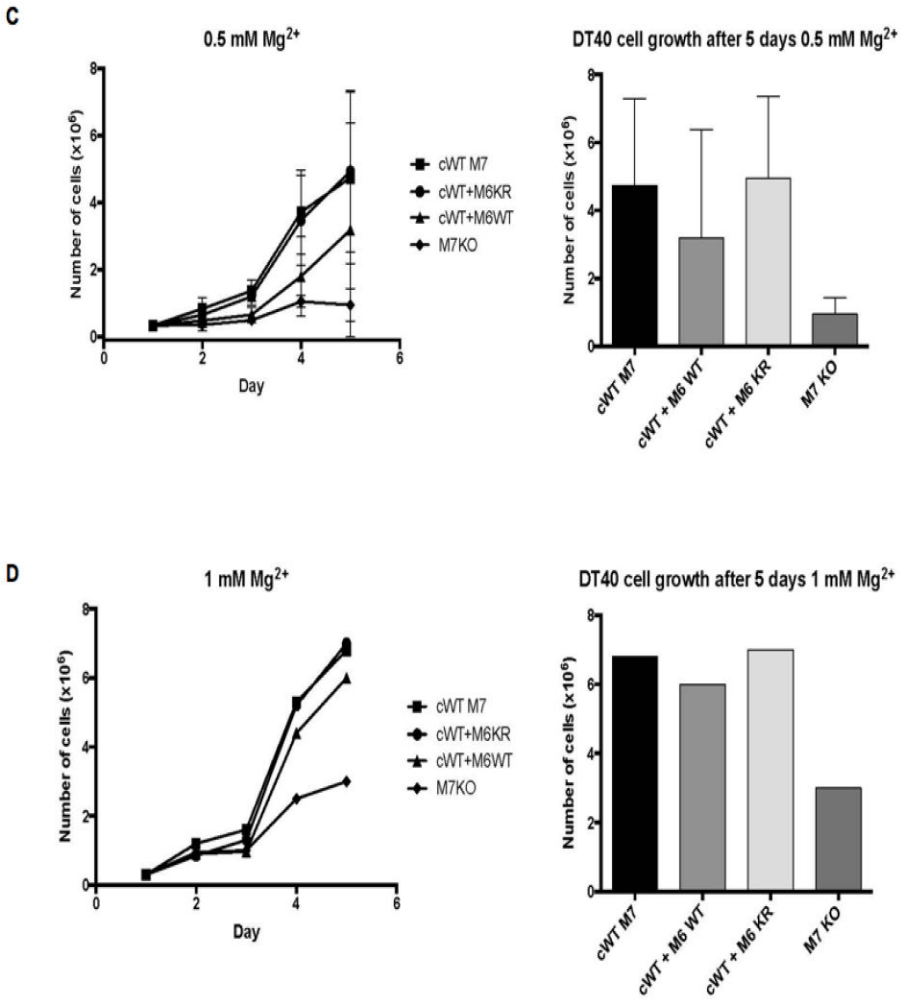

Figure 4. TRPM6 kinase activity inhibits TRPM7 mediated cell growth in HEK-293 and DT40 cells growth under hypomagnesic conditions

Fig. 4A, growth curves of HEK-293 expressing human TRPM7 WT (M7 WT) alone, or co-expressing hTRPM7 WT with either human TRPM6 WT (M6/7 WT), or the TRPM6 K1804R kinase dead mutant (M6KR + M7 WT). Cells were cultured in normal HEK-293 media, prior to Mg^{2+} deprivation protein overexpression was induced for 6h with doxycycline (1μg/ml). Cells were spun down and equal number of cells transferred for 24 hrs into fresh, complete, serum-free growth media with 0 or 1 mM Mg^{2+}, as indicated. Note: TRPM7 overexpressing HEK-293 cells die after 36-48 hrs doxycycline induced TRPM7 overexpression).

Fig. 4B-D, growth curves of TRPM7 deficient DT40 cells complemented with human TRPM7 WT (cWT M7) or cKR M7 (kinase dead) alone, or with hTRPM7 WT co-expressed with either human TRPM6 WT (cWT M7 + M6 WT), or the TRPM6 K1804R kinase dead mutant (cWT M7 + M6 KR). Cells were cultured in complete, chemically defined, Mg^{2+}-free media without serum requirement. Cells were grown under various Mg^{2+} concentrations for several days as indicated. Prior to Mg^{2+} deprivation protein overexpression has been induced for 24-48 hours with doxycycline (final concentration: 1μg/ml) in complete growth media with additional 10 mM $MgCl_2$ (Note: $TRPM7^{-/-}$ DT40 cells would die without Mg^{2+}

supplementation of the growth media). Cells were spun down and equal number of cells (2×10^5) transferred into fresh, complete growth media with different Mg^{2+} concentrations, as indicated. For statistical analysis, a two-tailed t-test was performed. Data shown are the mean ± SEM; *p< 0.05, **p<0.01,*** p<0.001. Note: Growth data at physiological (1mM Mg^{2+}) and hyerpmagnesic conditions have been published in 2003/2005 and did not show any differences.

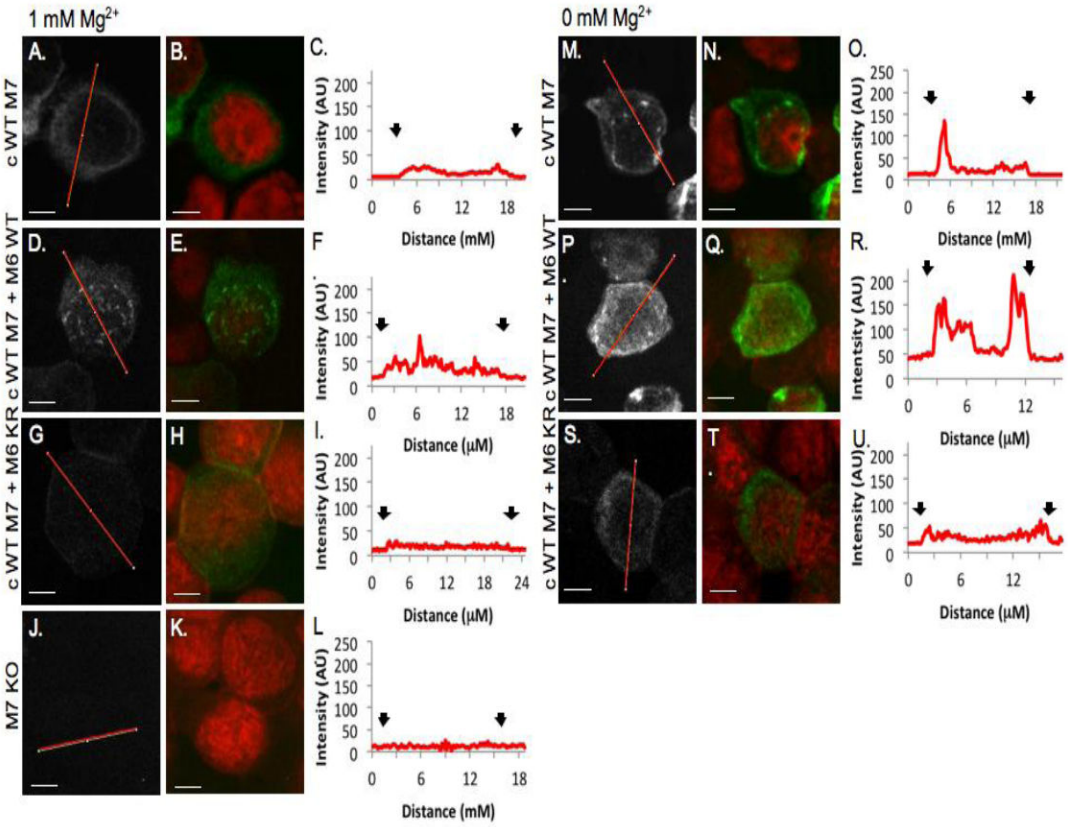

Figure 5. TRPM7 membrane trafficking pattern is altered by Mg^{2+} concentration and the TRPM6 kinase in DT40 B cells

100x confocal images of HA-tagged TRPM7 channels visualized with HA-FITC antibody (grey scale, green) and nuclei visualized with propidium iodide (red). Scale bars = 5 μM. TRPM7 $^{-/-}$ DT40 B cells complemented with human TRPM7 WT and co-expressing TRPM6 WT or TRPM6 KR grown in 1 mM Mg^{2+} (A-L) or 0 mM Mg^{2+} (M-U). Histograms correspond to one-pixel wide lines (red line in grey scale images) drawn across the center of the cell. A-C. cWT M7 cells in 1 mM Mg^{2+} TRPM7 immunoreactivity is diffuse throughout the cytoplasm with a small peak at the edge of the cell (black arrows, C.). D-F. TRPM7 immunoreactivity in 1 mM Mg^{2+} is also low and diffuse in cWT M7 + M6WT cells, except for the presence of TRPM7 clusters near the nuclear membrane. cWT M7 + M6 KR cells (J-L) express low levels of TRPM7 at 1 mM Mg^{2+}. In cells grown in 0 mM Mg^{2+}, TRPM7 immunoreactivity increases near the plasma and nuclear membranes in cWT M7 cells (M-U). cWT M7 + M6 KR cells have increased expression levels and clustered distribution of TRPM7 (P-R). There is a small increase in TRPM7 fluorescence near the periphery of cWT M7 + M6 KR cells (S-U). TRPM7 immunoreactivity is controlled for in TRPM7 $^{-/-}$ DT40 B cells that have no detectable fluorescence (J-L).